Critical behavior of the ideal-gas Bose-Einstein condensation in the Apollonian network

I. N. de Oliveira,[1] T. B. dos Santos,[1] F. A. B. F. de Moura,[1] M. L. Lyra,[1,2] and M. Serva[3,4]
[1]*Instituto de Física, Universidade Federal de Alagoas, 57072-970 Maceió, AL, Brazil*
[2]*Laboratoire de Physique de la Matière Condensée, UMR CNRS 7643, Ecole Polytechnique, 91128 Palaiseau, Cedex, France*
[3]*Departamento de Biofísica e Farmacologia, Universidade Federal do Rio Grande do Norte, 59072-970, Natal-RN, Brazil*
[4]*Dipartimento di Ingegneria e Scienze dell'Informazione e Matematica, Università dell'Aquila, 67010 L'Aquila, Italy*
(Received 5 February 2013; published 26 August 2013)

We show that the ideal Boson gas displays a finite-temperature Bose-Einstein condensation transition in the complex Apollonian network exhibiting scale-free, small-world, and hierarchical properties. The single-particle tight-binding Hamiltonian with properly rescaled hopping amplitudes has a fractal-like energy spectrum. The energy spectrum is analytically demonstrated to be generated by a nonlinear mapping transformation. A finite-size scaling analysis over several orders of magnitudes of network sizes is shown to provide precise estimates for the exponents characterizing the condensed fraction, correlation size, and specific heat. The critical exponents, as well as the power-law behavior of the density of states at the bottom of the band, are similar to those of the ideal Boson gas in lattices with spectral dimension $d_s = 2ln(3)/ln(9/5) \simeq 3.74$.

DOI: 10.1103/PhysRevE.88.022139 PACS number(s): 05.30.Jp, 67.85.Jk, 64.60.aq, 64.60.F−

I. INTRODUCTION

Bose-Einstein condensation (BEC) is one of the most remarkable quantum phenomena on which a macroscopic fraction of the bosonic particles constituting a physical system occupies a single quantum state, thus leading to the emergence of macroscopic spontaneous coherence. The production of gaseous BEC of cold weakly interacting atoms in a magnetic trap [1,2] represented a landmark in the physics history corroborating that the BEC is a purely quantum phenomenon that can take place even when interparticle interactions are negligible. Nowadays, BEC has also been reported in solid-state quasiparticles systems such as excitons, antiferro, and ferromagnetic magnons [3–6], which has stimulated additional studies concerning the universal features in the vicinity of the BEC transition.

The scaling behavior characterizing the Bose-Einstein condensation of an ideal gas has been a longstanding issue addressed by several authors in the framework of phase transitions and critical phenomena [7–12]. It has been demonstrated that there is a precise correspondence between the asymptotic properties of the thermodynamic quantities in the vicinity of the transition temperature and those of the spherical model of ferromagnetism [7]. Considering a single-particle density of states (DOS) having a power-law behavior DOS $\propto E^{\sigma}$ at the band bottom, the exponents characterizing the singular behavior of several quantities have been obtained [7,8], with $\sigma = d/2 - 1$ for particles enclosed in a d-dimensional box. One remarkable result is that the condensed fraction vanishes linearly as the reduced temperature $t = (T_c - T)/T_c \to 0$ irrespective to the value of σ, where T_c is the transition temperature below which a finite fraction of the particles condensate at the ground state. On the other hand, the correlation length diverges as $\xi \propto t^{-\nu}$, with $\nu = 1/2\sigma$ for $2 < d < 4$ and $\nu = 1/2$ for $d > 4$. The specific heat exponent is finite at the transition. For $d < 4$, the specific heat is continuous and a negative exponent $\alpha = -(1 - \sigma)/\sigma$ characterizes its cusp singularity, where $C_v(T) - C_v(T_c) \propto |t|^{-\alpha}$. For $d > 4$, it develops a jump discontinuity with $\alpha = -(\sigma - 1)$. At $d = 4$, a logarithmic singularity sets up in the specific heat. These exponents are modified by the presence of interparticle interactions. In particular, the condensed fraction decreases sublinearly, as reported in superfluid helium experiments [9].

In spite of the well-established critical behavior of the ideal gas BEC transition in homogeneous lattices, the corresponding scenario in complex inhomogeneous lattices is still under-explored. Within this context, exact analytical expressions for the thermodynamic properties of the ideal gas on the star and wheel networks have been recently reported [13]. The presence of a gap between the ground and excited states is responsible for the emergence of a low-temperature condensed phase, a feature also shared by networks composed of interconnected linear chains [14–18]. In the star and wheel networks, the critical behavior is mean-field-like. The condensed fraction vanishes linearly when approaching the transition, the specific heat is discontinuous, and the condensed fraction at the transition temperature scales with the number of lattice sites as $N^{-1/2}$.

BEC in scale-free networks are much less understood. These complex networks having a power-law distribution of site connectivity represent an important class of lattice models, which has contributed to the understanding of transport and information flow within systems of many degrees of freedom [19–23]. In this context, the deterministic Apollonian network has attracted much attention due to its scale-free and small-world properties [24–28]. The thermodynamic properties of the ideal electron gas on the Apollonian network reflects the complex structure of the single-particle DOS, such as the presence of δ-like singularities, gaps, and mini-bands [29,30]. On the other hand, when considering the same hopping amplitude between any pair of connected sites, the ideal boson gas was shown to present only a condensed phase in the thermodynamic limit, with no finite-temperature BEC transition [31]. This feature is related to the divergence of the ground-state energy with the network size due to the presence of sites with a diverging number of connections in the thermodynamic limit. Therefore, the actual critical behavior of the BEC transition of the ideal gas in scale-free networks is still an open issue.

Here, we fulfill this gap in the statistical mechanics description of the ideal boson gas by showing that a proper rescaling of the hopping couplings leads to a finite BEC transition temperature in the deterministic scale-free Apollonian network. After analytically demonstrating that the energy spectrum can be obtained from a nonlinear mapping, we will explore the scaling form of the condensed fraction density and specific heat in the vicinity of the transition to provide accurate estimates for some relevant critical exponents. In particular, we will show that the critical exponents, as well as the overall power-law behavior of the density of states near the band bottom, indicates that the BEC condensation in the Apollonian network belongs to the universality class of the ideal BEC in lattices with spectral dimension $d_s = 2ln(3)/ln(9/5) \simeq 3.74$.

II. TIGHT-BINDING HAMILTONIAN IN THE APOLLONIAN NETWORK

The Apollonian network in its two-dimensional version is generated recursively starting from a single equilateral triangle considered as generation $g = 0$. For the $(g + 1)$th generation, the network is obtained by inserting a site within each triangle of the gth generation, and connecting it to each of the triangle corners [see Fig. 1(a)]. The total number of network sites is then $N_g = (3^g + 5)/2$, while the total number of edges is $U_g = (3^{g+1} + 3)/2$. This network has a scale-free character. There are sites with distinct degrees of connectivity whose probability decays asymptotically as $p(k) \propto k^{-(1+\gamma)}$ with $\gamma = \ln 3/\ln 2 = 1.5849\ldots$.

We consider a tight-binding single-particle Hamiltonian in the above Apollonian network. Each site of the network will be considered as having a single orbital, whose onsite energy will be taken as $\epsilon_i = 0$ without loss of generality. Only first-neighbors hopping are included. Therefore the nondiagonal elements of the Hamiltonian matrix will be non-null only between directly connected sites. However, as the degree of connectivity of the network sites varies over a wide spectrum, each non-null off-diagonal element of the Hamiltonian matrix linking a pair of sites (i, j) will be rescaled by the geometric average of the connectivities of these two sites. In this way, the Hamiltonian assumes the form

$$H = \sum_{i,j}^{N} h_{i,j}|i\rangle\langle j|. \tag{1}$$

Here, $|i\rangle$ represents the state where the particle is localized at site i. The hopping amplitudes $h_{i,j} = h_{j,i}$ are non-null only between the connected sites of the network. We will consider two models; in model A it is assumed that the hopping energies are rescaled according to $h_{i,j} = t/\sqrt{k_i k_j}$, while in model B, such rescaling is slightly modified when the three sites at the corners are concerned as it will be explained in Sec. III. The parameter t is the only relevant microscopic energy scale while the rescaling of the off-diagonal Hamiltonian elements avoids the divergence of the ground-state energy while keeping the energy bandwidth finite in the thermodynamic limit. Rescaling of the microscopic energy scale is commonly used in model systems presenting highly connected sites in order to keep the thermodynamic limit well defined as, for example, in spin models with long-range connections [32–36]. The present procedure extends that employed in the study of BEC transition in the star and wheel networks [13].

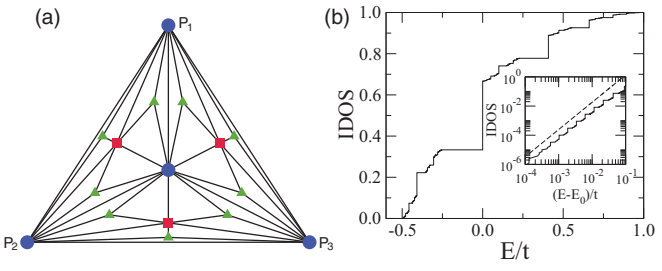

FIG. 1. (Color online) (a) Apollonian network with $g = 3$. P_1, P_2, and P_3 are the sites of the original triangle at the zeroth generation. (b) Integrated density of states (IDOS) within the tight-binding approximation for a single particle in an Apollonian network with $g = 15$ generations. Degenerescences and gaps are signaled by vertical and horizontal segments, respectively. The inset shows the power-law behavior near the band bottom IDOS $\propto (E - E_0)^{1+\sigma}$ [$1 + \sigma = \ln(3)/\ln(9/5) \simeq 1.87$] modulated by a fractal-like structure.

A. Exact mapping for the energy spectrum

Let us start by summarizing a few relevant properties of the Apollonian network:

(i) The number of sites at generation $g \geqslant 0$ is $N_g = (3^g + 5)/2$. For g large one has $N_g \sim 3^g/2$.

(ii) The number of new sites created at generation g is 3^{g-1} for $g > 0$, while the number of older sites is $(3^{g-1} + 5)/2 \sim 3^{g-1}/2$.

(iii) The number of sites with coordination k is $m(k,g)$, which equals 3^{s-1} if $k = 3 \cdot 2^{g-s}$ with $s = 1, \ldots, g$, equals 3 (the three corners) if $k = 1 + 2^g$ and equals 0, otherwise.

(iv) The number of edges at generation $g \geqslant 0$ is $U_g = (3^{g+1} + 3)/2$. For g large one has $U_g \sim 3^{g+1}/2$.

(v) The number of new edges created at generation g is 3^g for $g > 0$, while the number of older edges is $(3^g + 3)/2 \sim 3^g/2$.

We emphasize that, according to the above definitions, generation $g = 0$ corresponds to the network with 3 sites. Notice that for any g all newly created 3^{g-1} sites have coordination 3. Also notice that connectivity of older sites is increased by a factor 2 by generation upgrading with exception of the three corners (connectivity goes as $k = 1 + 2^g$).

In order to derive analytically the energy spectrum of the tight-binding Hamiltonian on the Apollonian network, we define two slightly different rescaling schemes for the hopping energies:

(A) Model A is defined assuming that hopping energies are $t/\sqrt{k_i k_j}$, where k_i and k_j are the connectivities of the two linked sites. In particular, the hopping energies connecting a corner to another site j are $t/\sqrt{(1 + 2^g)k_j}$, while the hopping energies connecting two corners are $t/(1 + 2^g)$.

(B) Model B differs from model A only because the hopping energies connecting a corner to another site j are $t/(\sqrt{2^g k_j})$, while the hopping energies connecting two corners are $t/2^{g+1}$. All the other hopping energies are $t/\sqrt{k_i k_j}$ as in model A.

Models A and B are identical in the thermodynamic limit ($g \to \infty$). Furthermore, their difference for finite values of g is very small since they differ only slightly for hopping energies concerning corner sites. Both models have $N_g = (3^g + 5)/2$ eigenvalues of the Hamiltonian. Model B has the relevant property that generation upgrading (from $g-1$ to g) modifies all hopping energies of older edges (included those edges linking corners) simply multiplying them by a factor $1/2$.

B. Eigenvalues of model *B*

In this subsection, we will assume $t = 1$ without loss of generality (in case $t \neq 1$ these eigenvalues must be simply multiplied by t). Model B at generation $g = 0$ is a fully connected three sites network with the three hopping energies all equal to $1/2$. The eigenvalues of the Hamiltonian are: $-1/2, -1/2, 1$.

Then, eigenvalues of generation g are obtained from eigenvalues of generation $g-1$ by the following rule:

(i) From any eigenvalue E' of the $N_{g-1} = (3^{g-1} + 5)/2$ eigenvalues of generation $g-1$, two rational numbers are generated by

$$E_{1,2} = \frac{1}{4}\left[E' \pm \sqrt{(E')^2 + \frac{8}{3}(2\,E' + 1)}\right], \qquad (2)$$

and, therefore, $2 \times N_{g-1}$ numbers are generated.

(ii) Among these $2 \times N_{g-1}$ numbers, only those which are nonvanishing are retained and they are all eigenvalues of generation g.

(iii) The list of the $N_g = (3^g + 5)/2$ eigenvalues of generation g is completed adding vanishing eigenvalues.

At generation $g = 1$, eigenvalues are: $-1/4, -1/4 - 1/2, 1$; at generation $g = 2$, there are 7 nonvanishing eigenvalues; while for generations $g \geqslant 2$, vanishing eigenvalues start to appear. In the thermodynamic limit, $1/3$ of the eigenvalues are vanishing.

C. Proof of the nonlinear mapping

Here, we will follow a recursive method similar to the one adopted in the past literature to determine the spectrum of harmonic excitations in hierarchical Sierpinski gaskets [37]. To proof the above nonlinear mapping for the energy spectrum of model B, we consider an older site (a site that is not newly created at last generation g). Let us call this site 0 and let us consider all its k_0 connected sites i; the local Schrödinger equation centered over site 0, correspondingly to an eigenvalue E, reads

$$E\,\psi_0 = \sum_{i=1}^{k_0} h_{0,i}\,\psi_i. \qquad (3)$$

Assume that site 0 is not a corner, then k_0 is even and among the k_0 connected sites there are $n_n = k_0/2$ newly created sites at generation g and $n_0 = k_0/2$ older sites. Let us assume that even values of i corresponds to newly created sites, then one has $h_{0,2i} = 1/\sqrt{3k_0}$, which implies $n_0\,(h_{0,2i})^2 = 1/6$.

Assume, on the contrary, that site 0 is a corner, then $k_0 = 2^g + 1$ is odd and among the $k_0 = 2^g + 1$ connected sites there are $n_n = 2^{g-1}$ newly created sites at generation g and $n_0 = 2^{g-1} + 1$ older sites (of which two are corners themselves). Let us again assume that even values of i corresponds to newly created sites, then one has $h_{0,2i} = 1/\sqrt{3 \times 2^g}$, which implies also in this case $n_0\,(h_{0,2i})^2 = 1/6$.

Let us now consider the n_n local Schrödinger equations centered over newly created sites connected to site 0. Let us use for them the even index $2i$, then for $2i = 2,4,\ldots 2\,n_n$, we have

$$E\,\psi_{2i} = h_{0,2i}\,\psi_0 + h_{2i-1,2i}\,\psi_{2i-1} + h_{2i+1,2i}\,\psi_{2i+1}, \qquad (4)$$

where, in the case that 0 is not a corner, we use the convention $\psi_{2n_n+1} = \psi_1$ and $h_{2n_n+1,2n_n} = h_{1,2n_n}$.

Assume that $E \neq 0$. In this case (and only in this case) the ψ_{2i} can be integrated; i.e., they can be substituted from Eq. (4) into Eq. (3). In this way, we obtain an equation that connects site 0 with sites with an odd i index, i.e., an equation which only concerns those n_0 older sites already existing at generation $g-1$.

We remark that $h_{j,2i}h_{0,2i} = \frac{1}{3}h_{j,0}$ always holds unless 0 and j are both corners; in this last case one has $h_{1,2i}h_{0,2i} = \frac{2}{3}h_{1,0}$ and $h_{2^g+1,2i}h_{0,2i} = \frac{2}{3}h_{2^g+1,0}$. Using these relations and the previously shown relation $n_n\,(h_{0,2i})^2 = 1/6$, which holds both if 0 is corner site or it is not, we straightforwardly obtain

$$\left(E - \frac{1}{6E}\right)\psi_0 = \sum_{i=1}^{n_o}\left(1 + \frac{2}{3E}\right)h_{2i-1,0}\,\psi_{2i-1}. \qquad (5)$$

The above equation, provided that $E \neq 0$, holds at any of the sites that were already present at generation $g-1$ and, therefore, it can be compared with the local Schrödinger equation centered on site 0 at generation $g-1$:

$$E'\,\psi_0 = \sum_{i=1}^{n_o} h'_{2i-1,0}\,\psi_{2i-1}. \qquad (6)$$

The hopping energies $h'_{2i-1,0}$ of model B at generation $g-1$ are twice the hopping energies $h_{2i-1,0}$ of generation g, then the two equations coincide provided that

$$2\left(E - \frac{1}{6E}\right) = E'\left(1 + \frac{2}{3E}\right), \qquad (7)$$

which immediately gives Eq. (2). Since the assumption was that $E \neq 0$, Eq. (2) only gives the nonvanishing eigenvalues of generation g, given the eigenvalues (vanishing and nonvanishing) of generation $g-1$. If there are missing eigenvalues after using Eq. (2), they must be vanishing eigenvalues. We finally remark that Eq. (2) maps real numbers in the interval $[-1/2,1]$ into real numbers in the same interval; therefore, since the three eigenvalues corresponding to $g = 0$ are in the interval, and at any generation only vanishing eigenvalues can be added, the density of states (DOS) must have a support contained in $[-1/2,1]$.

The integrated density of states (IDOS) for the generation $g = 15$ ($N = 7\,174\,456$ sites) is shown in Fig. 1(b) with eigenenergies ranging in a finite window from $-1/2 < E/t < 1$, contrasting with the diverging bandwidth that results when the off-diagonal terms are not properly rescaled [31]. The energy spectrum has a complex fractal-like aspect with degenerescences, gaps, and mini-bands with many distinct

scales. The inset shows a magnification of the IDOS near the band bottom $E_0 = -1/2$. Its presents an overall power-law behavior IDOS $\propto (E - E_0)^{1+\sigma}$ modulated by a scale invariant structure. The degradation very near the band bottom is a finite-size effect. The power-law exponent of the IDOS can be analytically derived from the exact iterative mapping for the energy eigenvalues given by Eq. (2). The eigenvalues close to the band bottom $E/t = -1/2$ at generation $g + 1$ came from eigen-energies that were close to the top of the band $E/t = 1$ at generation g. Linearizing relation Eq. (2) in the vicinity of $E/t = 1$, one obtains that the eigenstates that are at a small distance ε from the top of the band at generation $g - 1$ are compressed to a distance $5\varepsilon/9$ at generation g. Therefore, the total number of states close to the band bottom shall satisfy $N_{g-1}(\varepsilon) = N_g(5\varepsilon/9)$. Recalling that the total number of states grows by a factor 3 and assuming a power-law behavior of the IDOS at the band bottom, one directly obtains $1 + \sigma = \ln(3)/\ln(9/5) = 1.869\ldots$. The straight line in Fig. 1(b) represents such analytical scaling behavior and fits the overall initial growth of the IDOS.

III. THE BEC TRANSITION IN THE APOLLONIAN NETWORK

The above supralinear energy dependence of the IDOS at the band bottom points toward the occurrence of a BEC transition of the ideal boson gas with a fixed number N_p of particles. The thermodynamic properties in finite networks with g generations can be directly obtained from the corresponding energy spectrum. Within the framework of the grand canonical ensemble, the average number of particles at the ith energy state is given by

$$\langle n_i \rangle = \frac{1}{e^{\beta(E_i-\mu)} - 1} = \frac{1}{z^{-1}e^{\beta(E_i-E_0)} - 1}. \qquad (8)$$

Here, μ is the chemical potential and $\beta = 1/k_B T$. $z = e^{\beta(\mu - E_0)}$ is a properly defined fugacity that, in the thermodynamic limit of $g \to \infty$, shall become unit in the condensed phase. Following the standard grand-canonical ensemble procedure, the fugacity can be obtained as a function of temperature and particle density by imposing that $N_p = \sum_{i=1}^{N} \langle n_i \rangle$. Values of z were numerically computed with an accuracy of 10^{-12}.

In order to identify the occurrence of a BEC transition, we computed the average number of particles N_0 condensed in the ground state from $N_0 = z/(1 - z)$. In Fig. 2(a), we show the fraction of particles condensed in the ground state $\rho_0 = N_0/N_p$ as a temperature function for Apollonian networks with distinct generations. We considered a representative particle density $N_p/N = 1/2$. Except by a finite-size rounding off, a clear BEC transition develops at a finite temperature as the network size grows. The inset shows the same data near the transition in a universal finite-size scaling form (see following discussion). The dependence of the condensed fraction on temperature for distinct particle densities is shown in Fig. 2(b). As expected, the transition temperature is an increasing function of the particle density. Using a finite-size scaling approach (see following discussion) to precisely locate the transition temperature, we show in the inset its dependence on the particle density. It is straightforward to show that

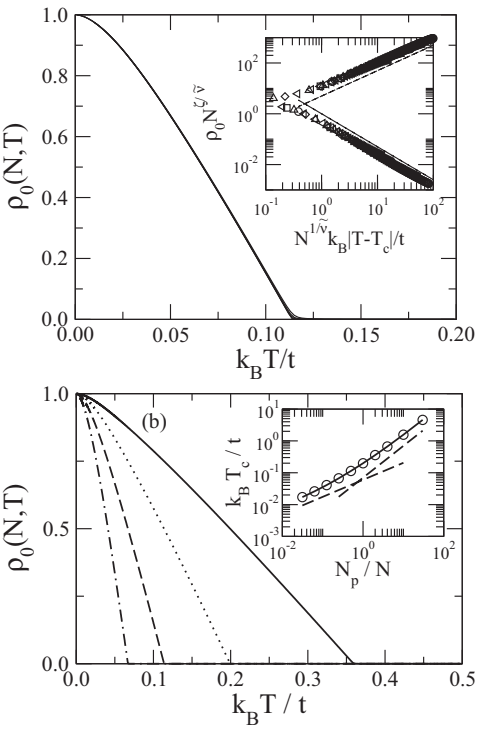

FIG. 2. (a) Condensed fraction N_0/N_p as a function of temperature for networks with distinct number of generations, $g = 11$ up to $g = 15$. Here, we used a particle density $N_p/N = 1/2$. The inset shows the data in a universal finite-size scaling form. The straight lines are consistent with the expected scaling behavior below and above the transition (see text); (b) Condensed fraction N_0/N_p as a function of temperature in a network with $g = 15$ generations and different particle densities: $N_p/N = 2$ (solid line), $N_p/N = 1$ (dotted line), $N_p/N = 1/2$ (dashed line), and $N_p/N = 1/4$ (dotted-dashed line). The inset shows the density dependence of the transition temperature T_c. The dashed lines correspond to the high density $T_c \propto N_p/N$ and low density $T_c \propto (N_p/N)^{1/(1+\sigma)}$ behavior.

the transition temperature grows linearly with N_p/N in the high-density regime. In the opposite regime of low densities, a slower $(N_p/N)^{1/(1+\sigma)}$ law sets up, according to the overall IDOS behavior near the band bottom.

The temperature dependence of the specific heat can also be used to signal the presence of the BEC transition. The specific heat at a constant particle density on a network with N sites can be written as $C_v = \partial U(N_p,T)/\partial T|_{N_p}$, where the internal energy $U(N_p,T) = \sum_{i=1}^{N} \varepsilon_i \langle n_i \rangle$. It is important to stress that the implicit dependence of the fugacity z on the temperature has to be taken into account. Figure 3 shows the specific heat per particle (in units of k_B) as a function of temperature for Apollonian networks with distinct number of generations and a fixed particle density $N_p/N = 1/2$. In the low-temperature regime, it displays a power-law behavior in the form $C_v \propto T^{1+\sigma}$, which is consistent with the main power-law vanishing of the density of states at the band bottom. Small deviations from the power-law regime at very low temperatures are due to finite-size effects, which are also evident near the peak signaling the BEC transition (shown in detail in the inset). Although the maximum specific heat

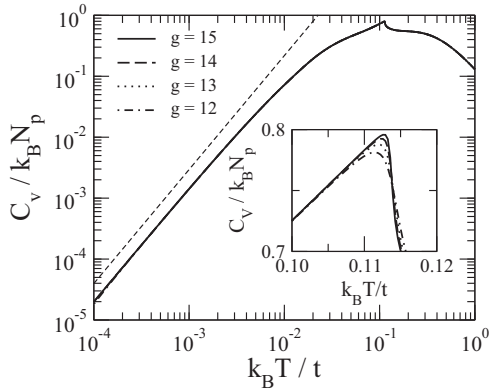

FIG. 3. The specific heat per particle (in units of k_B) as a function of temperature for a fixed particle density $N_p/N = 1/2$ in Apollonian networks with distinct number of generations. The low-temperature behavior $C_v \propto T^{1+\sigma}$ (shown as a straight dashed line) is consistent with the low-energy overall power-law behavior of the IDOS. Near the transition, the specific heat develops a peak rounded by finite-size effects. The data point toward a saturation of the peak height in the thermodynamic limit.

grows with the number of generations, the data point toward a saturation in the thermodynamic limit.

IV. FINITE-SIZE SCALING AND CRITICAL EXPONENTS

Finite-size scaling arguments can be put forward to accurately estimate the BEC transition temperature and the relevant critical exponents. Assuming a single-parameter scaling behavior, the condensed fraction in the vicinity of the transition shall have the universal form

$$\rho_0(N,T) = N^{-\zeta/\tilde{\nu}} h[(T - T_c)N^{1/\tilde{\nu}}], \tag{9}$$

where an implicit dependence on the particle density is assumed. ζ is the exponent governing the vanishing of the condensed fraction as the transition is approached from below [$\rho_0 \propto (T_c - T)^{\zeta}$] in the thermodynamic limit. $\tilde{\nu}$ is a typical correlation exponent that plays a role similar to $d\nu$ in regular d-dimensional lattices. There are several techniques that explore the above finite-size scaling hypothesis to compute the critical parameters. Here, we analyze the temperature dependence of the set of auxiliary functions

$$f(N,N',T) = \frac{\ln[\rho_0(N,T)/\rho_0(N',T)]}{\ln N/N'}, \tag{10}$$

computed for different pairs of network sizes (N,N'). According to the scaling hypothesis, these functions become independent of (N,N') at the transition temperature. Further, this scale invariant value of $f(N,N',T_c) = -\zeta/\tilde{\nu}$.

The critical exponents characterizing the BEC transition of the ideal Boson gas in dimension $d < 4$ are predicted to be $\zeta = 1$, $1/\tilde{\nu} = (d-2)/d$ [7,8]. The specific heat is also predicted to have a cusp singularity with and exponent $\alpha = -(4-d)/(d-2)$. In the following, we are going to show that these predictions hold for the Apollonian network when we consider that the overall power-law behavior of the IDOS can be associated to a spectral dimension $d_s = 2(1+\sigma) \simeq 3.74$. This is not to be confused with the standard fractal dimension

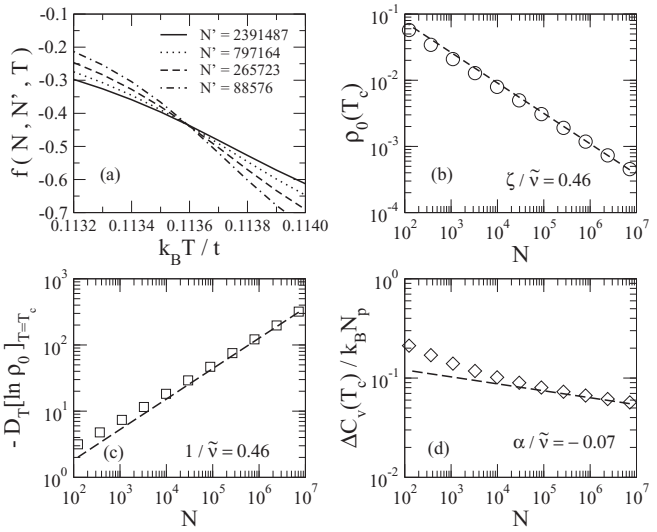

FIG. 4. (a) Auxiliary scaling functions $f(N,N',T)$ versus temperature using $N = 7\,174\,456$ ($g = 15$) and distinct values of N' ($g = 11,12,13$, and 14). Here, the particle density of $N/N_p = 1/2$ was used. The crossing point signals the BEC transition at $k_B T_c/t = 0.1136$. It is also shown the finite-size scaling of (b) the condensed fraction ρ_0, (c) its logarithmic derivative $\frac{d}{dT}\ln\rho_0(N,T)$, and (d) the specific heat singularity $C_v(N\to\infty) - C_v(N)$ at the transition temperature. The power-law scaling correspond $\zeta/\tilde{\nu} = 1/\tilde{\nu} = (d_s-2)/d_d \simeq 0.46$ and $\alpha/\tilde{\nu} = -(4-d_s)/d_s \simeq -0.07$.

of hierarchical lattices related to the growth of the number of sites with increasing system sizes. It has been evidenced that anomalous diffusion can be observed in systems presenting distinct values for the fractal and spectral dimensions [38,39]. The concept of spectral dimension is also important for several models of equilibrium statistical physics including Gaussian [40], spherical [41], and spin models [42,43]. The role played by the spectral dimension on the thermodynamic properties of the ideal Bose gas has been previously discussed in the literature, with emphasis to the occurrence of BEC only for $d_s > 2$ [15].

In Fig. 4(a), we show a set of auxiliary functions $f(N,N',T)$. In all of them we used N as the number of sites of the network with generation number $g = 15$ ($N = 7\,174\,456$), while N' was taken from networks with generation number ranging from $g = 11$ ($N' = 88\,576$) up to $g = 14$ ($N' = 2\,391\,487$). Here, we also considered a constant particle density $N_p/N = 1/2$. Notice that all curves cross roughly at the same point, thus indicating the BEC transition. Our best estimate for the transition temperature for this particular particle density is $k_B T_c/t = 0.1136$. In Fig. 4(b) we plot the condensed fraction at T_c for distinct network sizes. The scaling $\rho_0(N,T_c) \propto N^{-\zeta/\tilde{\nu}}$ holds for several orders of magnitudes of network sizes with some correction to scaling being present when networks with a small number of generations (typically $g \leqslant 10$) are considered. The straight line gives the predicted exponent $\zeta/\tilde{\nu} = (d_s-2)/d_s = 0.46\ldots$.

The correlation exponent $\tilde{\nu}$ can also be estimated by noticing that the derivative of the logarithmic of the condensed fraction with respect to temperature scales as $\frac{d}{dT}\ln\rho_0(N,T) \propto N^{1/\tilde{\nu}}$ at the transition. This scaling behavior is depicted in Fig. 4(c) together with the predicted power-law behavior

with exponent $1/\tilde{\nu} = (d_s - 2)/d_s \simeq 0.46$. In order to test the accuracy of the above critical parameters, we plotted the condensed fraction data reported in the main frame of Fig. 2(a) in a properly scaled form, namely $N^{\zeta/\tilde{\nu}}\rho_0$ versus $N^{1/\tilde{\nu}}k_B|T - T_c|/t$. According to the finite-size scaling hypothesis, data from distinct network sizes shall collapse into a single curve when the appropriate critical parameters are used. The data collapse in the condensed phase is shown in the inset of Fig. 2(a), on which the above values for the critical temperature and exponents were used. The collapse is quite impressive, thus supporting the accuracy of the present critical parameters. It is interesting to notice that the present results indicate the condensed fraction vanishes linearly as the BEC transition is approached $\zeta = 1$. This linear scaling-law is shown as the straight upward dashed line in the inset of Fig. 2(a) and fits perfectly well the collapsed data. This feature is consistent with the value $\zeta = 1$ for the BEC transition of the ideal gas in lattice models with a pure power-law vanishing of the DOS at the band bottom [7,8]. The downward dashed straight line has a slope consistent with the $1/N$ vanishing of the condensed fraction above the transition temperature.

Finally, similar finite-size scaling arguments can be used to analyze the specific heat data. At the transition temperature, the data reported in Fig. 3 indicates that $C_v(N \to \infty, T_c)$ converges to a finite value, a feature shared by the ideal gas BEC transition in regular lattices. The singular part of the specific heat $C_v(N \to \infty, T) - C_v(N, T)$ also obeys a single-parameter scaling form. At the critical point, it scales as $C_v(N \to \infty, T_c) - C_v(N, T_c) \propto N^{-\alpha/\tilde{\nu}}$. The size dependence of the singular contribution to the specific heat at the critical point is shown in Fig. 4(d) for a particle density $N_p/N = 1/2$ for which our best estimate was $C_v(N \to \infty, T_c)/k_B N_p = 0.813$. We also show the predicted asymptotic power-law scaling with exponent $\alpha/\tilde{\nu} = -(4 - d_s)/d_s \simeq -0.07$. Together with the previous value of the correlation exponent, this last result implies in $\alpha \simeq -0.15$. The hyperscaling relation $\tilde{\nu} = 2 - \alpha$ is satisfied.

V. SUMMARY AND CONCLUSIONS

In conclusion, we showed that a finite-temperature BEC transition of the ideal boson gas takes place in scale-free networks when the off-diagonal elements of the one-particle Hamiltonian are properly normalized by the geometric average of the sites connectivities. We illustrated this feature by computing the thermodynamic properties of the ideal gas on the Apollonian network due to its deterministic nature and simultaneous scale-free and small-world characteristics. The one-particle energy spectrum has an overall power-law behavior at the band bottom modulated by a fractal-like structure signaling the hierarchical topology of the underlying complex network. We analytically showed that the energy spectrum can be obtained from a nonlinear mapping. A finite-size scaling analysis of the condensed fraction and specific heat near the transition temperature was employed to provide accurate estimates of three critical exponents. Strong corrections to scale are present, particularly in the order parameter density and specific heat in networks with a small number of generations ($g < 10$). The asymptotic power-law behavior was probed using networks with sizes ranging from 10^5 up to 10^7 sites. Such large network sizes could only be addressed due to the analytical derivation of the energy spectrum. A collapse of data from networks with distinct sizes corroborates the estimated critical parameters. In particular, the condensed fraction was found to vanish linearly as the transition is approached, in agreement with the behavior near the ideal gas BEC transition in regular lattices. Further, the hyperscaling relation between the correlation and specific heat critical exponents was verified. All results indicate that the BEC transition in the Apollonian networks belongs to the universality class of the ideal gas BEC in lattices with spectral dimension $d_s = 2ln(3)/ln(9/5) \simeq 3.74$. A systematic exploration of the ideal boson gas in distinct topologies would be in order to elucidate the specific role played by scale-free, small-world, and hierarchical properties of complex networks on the universal behavior of the BEC transition.

ACKNOWLEDGMENTS

This work was partially financed by the Brazilian Research Agencies CAPES, CNPq, FINEP, and FAPEAL. M.L.L. acknowledges the hospitality of the Condensed Matter Physics group at Ecole Polytechnique, where part of this work was developed.

[1] M. H. Anderson, J. R. Ensher, M. R. Matthews, C. E. Wieman, and E. A. Cornell, Science **269**, 198 (1995).
[2] K. B. Davis, M.-O. Mewes, M. R. Andrews, N. J. van Druten, D. S. Durfee, D. M. Kurn, and W. Ketterle, Phys. Rev. Lett. **75**, 3969 (1995).
[3] L. V. Butov, C. W. Lai, A. L. Ivanov, A. C. Gossard, and D. S. Chemla, Nature (London) **417**, 47 (2002).
[4] J. Kasprzak, M. Richard, S. Kundermann, A. Baas, P. Jeambrun, J. M. J. Keeling, F. M. Marchetti, M. H. Szymańska, R. André, J. L. Staehli, V. Savona, P. B. Littlewood, B. Deveaud, and Le Si Dang, Nature (London) **443**, 409 (2006).
[5] T. Giamarchi, C. Rüegg, and O. Tchernyshyov, Nature Phys. **4**, 198 (2008).
[6] S. O. Demokritov, V. E. Demidov, O. Dzyapko, G. A. Melkov, A. A. Serga, B. Hillebrands, and A. N. Slavin, Nature (London) **443**, 430 (2006).
[7] J. D. Gunton and M. J. Buckingham, Phys. Rev. **166**, 152 (1968).
[8] C. K. Hall, J. Stat. Phys. **13**, 157 (1975).
[9] B. C. Crooker, B. Hebral, E. N. Smith, Y. Takano, and J. D. Reppy, Phys. Rev. Lett. **51**, 666 (1983).
[10] P. B. Weichman, M. Rasolt, M. E. Fisher, and M. J. Stephen, Phys. Rev. B **33**, 4632 (1986).
[11] V. C. Aguilera-Navarro, M. de Llano, and M. A. Solís, Eur. J. Phys. **20**, 177 (1999).
[12] L. Ferrari, Eur. J. Phys. **32**, 1547 (2011).

[13] E. J. G. G. Vidal, R. P. A. Lima, and M. L. Lyra, Phys. Rev. E **83**, 061137 (2011).
[14] R. Burioni, D. Cassi, I. Meccoli, M. Rasetti, S. Regina, P. Sodano, and A. Vezzani, Europhys. Lett. **52**, 251 (2000).
[15] R. Burioni, D. Cassi, M. Rasetti, P. Sodano, and A. Vezzani, J. Phys. B: At. Mol. Opt. Phys. **34**, 4697 (2001).
[16] P. Buonsante, R. Burioni, D. Cassi, and A. Vezzani, Phys. Rev. B **66**, 094207 (2002).
[17] I. Brunelli, G. Giusiano, F. P. Mancini, P. Sodano, and A. Trombettoni, J. Phys. B: At. Mol. Opt. Phys. **37**, 275 (2004).
[18] P. Sodano, A. Trombettoni, P. Silvestrini, R. Russo, and B. Ruggiero, New J. Phys. **8**, 327 (2006).
[19] R. Sharan and T. Ideker, Nat. Biotechnol. **24**, 427 (2006).
[20] S. Wassermann and K. Faust, *Social Network Analysis* (Cambridge University Press, Cambridge, 1994).
[21] R. Cohen, K. Erez, D. ben-Avraham, and S. Havlin, Phys. Rev. Lett. **85**, 4626 (2000).
[22] R. Cohen, K. Erez, D. ben-Avraham, and S. Havlin, Phys. Rev. Lett. **86**, 3682 (2001).
[23] A. A. Moreira, J. S. Andrade, and L. A. Nunes Amaral, Phys. Rev. Lett. **89**, 268703 (2002).
[24] J. S. Andrade, H. J. Herrmann, R. F. S. Andrade, and L. R. da Silva, Phys. Rev. Lett. **94**, 018702 (2005).
[25] J. P. K. Doye and C. P. Massen, Phys. Rev. E **71**, 016128 (2005).
[26] A. A. Moreira, D. R. Paula, R. N. Costa Filho, and J. S. Andrade, Jr., Phys. Rev. E **73**, 065101 (2006).
[27] P. G. Lind, L. R. da Silva, J. S. Andrade, Jr., and H. J. Herrmann, Phys. Rev. E **76**, 036117 (2007).
[28] C. N. Kaplan, M. Hinczewski, and A. N. Berker, Phys. Rev. E **79**, 061120 (2009).
[29] A. L. Cardoso, R. F. S. Andrade, and A. M. C. Souza, Phys. Rev. B **78**, 214202 (2008).
[30] I. N. de Oliveira, F. A. B. F. de Moura, M. L. Lyra, J. S. Andrade, Jr., and E. L. Albuquerque, Phys. Rev. E **79**, 016104 (2009).
[31] I. N. de Oliveira, F. A. B. F. de Moura, M. L. Lyra, J. S. Andrade, Jr., and E. L. Albuquerque, Phys. Rev. E **81**, 030104 (2010).
[32] M. Caffarel and W. Krauth, Phys. Rev. Lett. **72**, 1545 (1994).
[33] A. Georges, G. Kotliar, W. Krauth, and M. J. Rozenberg, Rev. Mod. Phys. **68**, 13 (1996).
[34] R. J. Baxter, *Exactly Solved Models in Statistical Mechanics* (Academic Press, London, 1982).
[35] M. Antoni and S. Ruffo, Phys. Rev. E **52**, 2361 (1995).
[36] C. Anteneodo and C. Tsallis, Phys. Rev. Lett. **80**, 5313 (1998).
[37] R. Rammal, J. Physique **45**, 191 (1984).
[38] S. Alexander and R. Orbach, J. Physique Lett. **43**, L623 (1982).
[39] R. Rammal, J. Stat. Phys. **36**, 547 (1984).
[40] K. Hattori, T. Hattori, and H. Watanabe, Prog. Theor. Phys. Suppl. **92**, 108 (1987).
[41] D. Cassi and L. Fabbian, J. Phys. A **32**, L93 (1999).
[42] D. Cassi, Phys. Rev. Lett. **76**, 2941 (1996).
[43] R. Burioni, D. Cassi, and A. Vezzani, Phys. Rev. E **60**, 1500 (1999).